Line mixing in the $\nu 6$ Q branches of self- and nitrogen-broadened methyl bromide

Ha Tran, David Jacquemart, Jean-Yves Mandin, Nelly Lacome

Line mixing in the ν_6 *Q* branches of self- and nitrogen-broadened methyl bromide

H. Tran [a], D. Jacquemart [b,*], J.-Y. Mandin [a], N. Lacome [b]

[a] *Université Pierre et Marie Curie-Paris 6; CNRS; Laboratoire de Physique Moléculaire pour l'Atmosphère et l'Astrophysique (LPMAA), UMR 7092, Case courrier 76, 4, place Jussieu, 75252 Paris Cedex 05, France*

[b] *Université Pierre et Marie Curie-Paris 6; CNRS; Laboratoire de Dynamique, Interactions et Réactivité (LADIR), UMR 7075, Case courrier 49, Bât F 74, 4, place Jussieu, 75252 Paris Cedex 05, France*

Received 2007

* Corresponding author. Tel.: + 33-1-44-27-36-82; fax: + 33-1-44-27-30-21.
E-mail address: jacquemart@spmol.jussieu.fr.

Abstract

Line-mixing effects are studied in the ν_6 $^{R}Q_K$ and $^{P}Q_K$ (K = 0 - 6) branches of CH_3Br perturbed by nitrogen. Laboratory Fourier transform spectra have been obtained at room temperature, and for a large range of pressure values of atmospheric interest. In order to accurately model these spectra, a theoretical approach accounting for line-mixing effects is proposed. This model is based on the use of the state-to-state rotational cross-sections calculated by a statistical modified exponential-gap fitting law depending on a few empirical parameters. These parameters are deduced adjusting the calculated diagonal elements of the relaxation matrix to the N_2-broadening coefficients, known from accurate previous measurements. Comparisons between experimental and calculated profiles for various Q branches and under various pressure conditions (0.2 - 1 atm), demonstrate the adequacy and consistency of the proposed model. To allow accurate laboratory measurements, line-mixing effects are also modeled in the case of self-perturbed CH_3Br.

Key words: Methyl bromide; Fourier transform spectroscopy; Infrared; Vibration-rotation; Line mixing

1. Introduction

Methyl bromine (CH_3Br) is the major source of stratospheric bromide, which has been shown to contribute significantly to the ozone depletion. It is also the primary organobromide species in the lower atmosphere. For these reasons, the infrared spectrum of CH_3Br has been extensively studied in the 10 µm atmospheric window, where the fundamental ν_6 band occurs (see Refs. [1,2] and references therein). In 2002, Brunetaud et al [1] studied line positions and intensities for the two main isotopologues $CH_3{}^{79}Br$ and $CH_3{}^{81}Br$, and generated a synthetic spectrum between 820 and 1120 cm^{-1}, for atmospheric purposes. Recently, Jacquemart et al [2] studied again this spectral region, measuring a larger number of line positions and intensities, as also numerous N_2- and self-broadening coefficients at room temperature. A more accurate theoretical treatment of the Hamiltonian and dipole moment operators has also been performed, allowing the calculation of a line list (about 15000 lines of both isotopologues) dedicated to atmospheric databases.

As *Q* branches of the ν_6 band are the best candidates for atmospheric remote sensing, they have to be known as accurately as possible. Previous studies [2] were limited to relatively low pressures (smaller than 30 hPa). In the present work, nitrogen pressures up to about 1 atm were used. In such conditions, the usual Voigt or Lorentz line profiles can no longer correctly reproduce the experimental shape of the *Q* branches, because of line mixing [3,4]. Line mixing has been studied for various molecules as CO_2, N_2O, CH_4. For C_{3v} molecules, the number of works is less. The line-mixing effects have been analyzed for CH_3F perturbed by rare gas [5,6] using a dynamical model. A simple modelling of the ν_5 $^RQ_0$ branch of CH_3Cl perturbed by N_2 was proposed by Hartmann et al [7] and Frichot et al [8]. Lately, a statistical model was used by Chackerian et al to calculate this *Q* branch [9]. In the present paper, a model similar to the one used for CH_3Cl [9] was applied to calculate line mixing in the ν_6 ^RQ_K and ^PQ_K (K = 0 - 6) branches of CH_3Br perturbed by nitrogen and self perturbed.

In this aim, laboratory Fourier transform spectra have been obtained at room temperature, and for a large range of pressure values of atmospheric interest (0.2 - 1 atm). Spectra and experimental considerations are presented in Section 2. A model based on the use

of the state-to-state rotational cross-sections, calculated by a statistical modified exponential-gap fitting law depending on a few empirical parameters, was used to model line mixing. The parameters were deduced through a sum rule, adjusting the diagonal elements of the relaxation matrix to the N_2-broadening coefficients, previously measured [2]. This model is presented in Section 3, together with the spectroscopic parameters used to calculate the CH_3Br spectra. Comparison between experimental and calculated spectra for various *Q* branches is discussed in Section 4. Line-mixing effects modeled in the case of self-perturbed CH_3Br, are also presented in the same section.

2. Experiment

The rapid scan Bruker IFS 120 HR interferometer of the Laboratoire de Dynamique, Interactions et Réactivité (LADIR) was used to record self- and N_2-perturbed spectra of CH_3Br. The unapodized spectral resolution (FWHM) used is ranging from about 1 to 4×10^{-3} cm^{-1}, corresponding to a maximum optical path difference ranging from 125 to 400 cm. The interferometer was equipped with a Ge/KBr beamsplitter, a MCT photovoltaic detector, a Globar source, and an optical filter covering the 800 - 1100 cm^{-1} spectral region. The experimental conditions of the recorded spectra are summarized in Table 1. Under these conditions, the rotational structure of CH_3Br transitions is not completely resolved, as it can be observed on Fig. 1 which presents the whole studied spectral domain. For all spectra, the whole optical path was under vacuum. Two cells were used: a multipass cell of 1 m base length with a total absorption path of 415 cm, as well as a 30 cm cell. These cells were equipped with KCl windows. The commercial gas sample, furnished by Fluka, with a stated purity of 99.50% in natural abundances, was used without further purification. All the spectra recorded in this work are at room temperature, close to 296 K. The pressure of the gas was measured with a capacitance MKS Baratron manometer with an accuracy estimated to be ±1%. Every scan among the 200 recorded for each spectrum has then been individually transformed to spectrum, using the Fourier transform procedure included in the Bruker software OPUS package [10], selecting a Mertz phase error correction [11,12]. The spectra were not numerically apodized. They were slightly over sampled (over sampling ratio equal to 2) by post-zero filling the interferograms. Averaging the 200 scans, the signal to noise ratio is

nearly equal to 100. Symmetric line profiles were observed on the average spectra, validating that the phase error was well corrected. Note that, as for spectra of Ref. [2], a weak multiplicative channelled spectrum is expected in the experimental spectra. Due to the high pressure of gases used in this work, it is more difficult to remove this channelled spectrum. The residuals of the adjustments on Fig. 1 give an idea of its amplitude, especially around 1000 cm^{-1} where it is the strongest.

Though the line-mixing of CH_3Br self-perturbed has no importance for atmospheric applications and could be neglected in our spectra, its knowledge is useful for laboratory experiments that require noticeable CH_3Br concentrations. Therefore, a few pure CH_3Br spectra were recorded under pressures up to about 100 hPa.

3. Theoretical model

This section is dedicated to the theoretical treatment of the CH_3Br line-mixing. Sections 3.1 and 3.2 are devoted to the formulation of the absorption coefficient and of the relaxation operator, and the application of this model is described in Section 3.3.

3.1. Absorption coefficient

Let us consider a mixture of an absorbing gas and of a buffer gas. Within the impact and binary collisions approximations, and disregarding Doppler effect that has negligible influences in the studied pressure range, the absorption coefficient α, in cm^{-1}, accounting for line-mixing effects at wavenumber σ and for temperature T is given by [3,4]

$$\begin{aligned}\alpha(\sigma, P_{\text{abs}}, P_{\text{buffer}}, T) &= \frac{8\pi^2\sigma}{3hc}\left[1-\exp(-hc\sigma/k_BT)\right] \\ &\times P_{\text{abs}}\sum_k\sum_\ell \rho_k(T)d_k d_\ell \,\text{Im}\left\langle\!\left\langle \ell \left| \left[\boldsymbol{\Sigma} - \mathbf{L_0} - \text{i}\left(P_{\text{abs}}\times\mathbf{W}_{\text{abs/abs}}(T) + P_{\text{buffer}}\times\mathbf{W}_{\text{abs/buffer}}(T)\right)\right]^{-1}\right| k\right\rangle\!\right\rangle.\end{aligned} \quad (1)$$

In this equation, P_{abs} and P_{buffer} are the partial pressures of the absorbing and buffer gases, respectively. The sums include all absorption lines k and ℓ, Im{…} denotes the imaginary

part, ρ_k is the fractional population of the initial level of line *k*, and d_n is the reduced matrix element of the electric dipole moment operator of line *n* (*n* = ℓ or *k*), related to the integrated line intensity S_n of the absorbing gas by

$$S_n(T) = \frac{8\pi^3}{3hc}\rho_n(T)\times\sigma_n\times\left[1-\exp\left(hc\sigma_n / k_B T\right)\right]\times d_n{}^2 \ . \qquad (2)$$

Σ, $\mathbf{L_0}$ and **W** are operators in the Liouville line space. The first two are diagonal and can be expressed as follows:

$$\left\langle\left\langle \ell\left|\mathbf{\Sigma}\right|k\right\rangle\right\rangle = \sigma_k\times\delta_{k,\ell} \text{ and } \left\langle\left\langle \ell\left|\mathbf{L}_0\right|k\right\rangle\right\rangle = \sigma_k\times\delta_{k,\ell}\,, \qquad (3)$$

$\delta_{k,\ell}$ being the Kronecker symbol.

The relaxation operators $\mathbf{W}_{\text{abs/abs}}$ and $\mathbf{W}_{\text{abs/buffer}}$, which contain the influence of collisions on the spectral shape, depend on the band, on the temperature, and on the collision partners. The off-diagonal elements of **W** account for interferences between absorption lines (line mixing), whereas the real and imaginary parts of the diagonal elements are the pressure-broadening (γ_k) and pressure-shifting (δ_k) coefficients of the lines

$$\left\langle\left\langle k\left|\mathbf{W}(T)\right|k\right\rangle\right\rangle = \gamma_k(T) - \mathrm{i}\delta_k(T)\,. \qquad (4)$$

In the case of $\mathbf{W}_{\text{abs/abs}}$, γ_k and δ_k are the self-broadening and -shifting coefficients of the absorbing transitions, whereas for $\mathbf{W}_{\text{abs/buffer}}$, γ_k and δ_k are the broadening and shifting coefficients due to the pressure of the buffer gas. Let us recall that neglecting line mixing (i.e., assuming that all off-diagonal elements of **W** are equal to zero) leads to express the profile as a sum of Lorentz profiles.

3.2. Relaxation operator

According to Eq. (4), the diagonal elements are set to the broadening and shifting coefficients. The imaginary part of the off-diagonal elements can be neglected, since the shifting coefficients are expected to be small, as it has been shown experimentally [2]. The real off-diagonal elements are modeled using the state-to-state inelastic collisional rates of the lower state through

$$\langle\langle \ell | \mathbf{W}(T) | k \rangle\rangle = -A_{\ell,k} \times K(i_\ell \leftarrow i_k, T) \quad \text{, with } (k \neq \ell), \tag{5}$$

where $K(i_\ell \leftarrow i_k, T)$ designates the state-to-state collisional transfer rate from the initial level i_k of line k to the initial level i_ℓ of line ℓ, at temperature T. The parameters $A_{\ell,k}$, which enable switching from the state-space to the line-space, are empirical and depend on the types of lines k and ℓ considered [13,14]. In order to simplify the problem, we made the approximation that $A_{\ell,k}$ depends only on the band and on the buffer gas, but not on the quantum numbers of the lines themselves.

The downward rates $K(i_\ell \leftarrow i_k, T)$, with $E_\ell < E_k$, are modeled by a statistical modified exponential-gap (MEG) fitting law [4,9,15]

$$K(i_\ell \leftarrow i_k, T) = a_1 \left(\frac{1 + a_4 (E_k / a_2 k_B T)}{1 + a_4 (E_k / k_B T)} \right)^2 \exp\left(- \frac{a_3 |E_k - E_\ell|}{k_B T} \right) \quad , \tag{6}$$

where E_n is the rotational energy of the initial level of line n ($n = \ell$ or k). The upward rates are then calculated by using the detailed balance

$$K(i_k \leftarrow i_\ell, T) = K(i_\ell \leftarrow i_k, T) \times \rho_k(T) / \rho_\ell(T) \, . \tag{7}$$

The coefficients a_1, a_2, a_3, and a_4 are obtained by least squares fitting the sum rule to the $\gamma(k)$ values. For a Q branch, this sum rule is modeled by

$$\gamma(k) = \frac{1}{2}\left(\sum_{J_\ell \neq J_k} K(i_\ell \leftarrow i_k) + \sum_{J'_\ell \neq J'_k} K(f_\ell \leftarrow f_k)\right), \quad (8)$$

where i_n and f_n are respectively the initial and final level of the transition n ($n = \ell$ or k), J_n and J'_n are the rotational quantum numbers of i_n and f_n.

3.3. Application to the CH_3Br spectra

Using experimental spectra recorded at various CH_3Br and N_2 pressures, we calculated the effects of line mixing, due to both CH_3Br and N_2, in several *Q* branches of the ν_6 band. As *Q* branches are well separated (see Fig. 1), inter-branch line mixing (for example with $\Delta K = 3n$ [16]) have not been taken into account.

The spectroscopic parameters required for the calculation of the profiles at room temperature are σ_k, ρ_k, d_k, E_k, γ_k. All these parameters have been constrained to the values obtained in Ref. [2]. As it has been said previously, the pressure shift has been neglected. Note that neglecting them has no observable consequence in the calculated spectra. The pressure of the absorbing gas is the partial pressure of one of the two main isotopologues, i.e, $CH_3{}^{79}Br$ or $CH_3{}^{81}Br$, whose concentration (in natural abundances) are 50.54 % and 49.46 % respectively. The concentration of the ^{13}C isotopologues (about 1 % on the whole) is neglected. As these two isotopologues have similar abundances and absorb in the same spectral region, they have to be studied simultaneously, so that the whole absorption coefficient is actually the sum of the absorption coefficients due to each isotopologue. Note that the line intensity in Eq. (2) is defined for a 100% $CH_3{}^{79}Br$ or $CH_3{}^{81}Br$ sample, not to be confused with that given in natural abundances [2].

For the calculation of the off-diagonal elements of the relaxation operators $\mathbf{W}_{CH_3Br/CH_3Br}$ and $\mathbf{W}_{CH_3Br/N_2}$, the parameters a_1, a_2, a_3, and a_4 have been determined through a sum rule from a least-squares fit of the self- and N_2-broadening coefficients respectively. For this treatment, the smoothed values of the measured data determined in Ref. [2] were chosen, instead of the measured values. Since in this previous work the N_2-broadening coefficients of

$CH_3{}^{79}Br$ and $CH_3{}^{81}Br$ were found very close, the same smoothed N_2-broadening coefficients were given for both $CH_3{}^{79}Br$ and $CH_3{}^{81}Br$ isotopologues. Then, the a_1, a_2, a_3, and a_4 parameters were supposed to be the same for the two isotopologues. However, as other spectroscopic data (σ_k, ρ_k, d_k, γ_k) are different for the two isotopologues, the state-to-state collisional transfer rates were evaluated separately for these two molecules. That is to say, we calculated a relaxation operator $\mathbf{W}_{CH_3Br/CH_3Br}$ for each isotopologue, noted $\mathbf{W}_{CH_3{}^{79}Br/CH_3Br}$ and $\mathbf{W}_{CH_3{}^{81}Br/CH_3Br}$, we also assumed that $\mathbf{W}_{CH_3{}^{79}Br/CH_3{}^{79}Br} = \mathbf{W}_{CH_3{}^{79}Br/CH_3{}^{81}Br}$, noted $\mathbf{W}_{CH_3{}^{79}Br/CH_3Br}$, and $\mathbf{W}_{CH_3{}^{81}Br/CH_3{}^{79}Br} = \mathbf{W}_{CH_3{}^{81}Br/CH_3{}^{81}Br}$, noted $\mathbf{W}_{CH_3{}^{81}Br/CH_3Br}$.

The parameters a_1, a_2, a_3, and a_4 obtained for the ${}^RQ_0$ branch were retained for all the other Q branches, since it is the strongest of the observed branches, and therefore is the most tractable to derive significant line-mixing parameters. We checked that the values found for the parameters from the ${}^RQ_0$ branch can be transferred for others branches without degrading the residuals. Moreover, before calculating the absorption coefficient, a renormalization procedure [17] has been applied to the off-diagonal terms of $\mathbf{W}$, in order to satisfy almost exactly the sum rule (Eq. 8).

For the ${}^RQ_0$ branch, the sum rule was evaluated with unrestricted collisional selection rules on ΔJ with $J \leq 59$ (broadening coefficients being known up to $J = 59$) and with $\Delta K = 0$ [16,18-20]. The vibrational ground state has only A+ levels. The upper states of ν_6 ${}^RQ_0$ transitions are split into A– and A+ levels. The optical selection rule for these ${}^RQ_0$ transitions is A+ $\rightarrow$ A–. As mentioned by Chackerian et al [9], who studied the CH_3Cl molecule similar to CH_3Br, both collisional relaxation between A– $\leftrightarrow$ A– and A– $\leftrightarrow$ A+ levels (instead of only A– $\leftrightarrow$ A–) in the excited state were needed to correctly describe line-mixing effects in CH_3Cl. Allowing also such collisional relaxations for CH_3Br, the sum rule becomes

$$\gamma(k) = \frac{1}{2}\left(\sum_{\substack{J_\ell \neq J_k \\ A+\leftrightarrow A+}} K(i_\ell \leftarrow i_k) + \frac{1}{2}\sum_{\substack{J'_\ell \neq J'_k \\ A-\leftrightarrow A-}} K(f_\ell \leftarrow f_k) + \frac{1}{2}\sum_{\substack{J'_\ell \neq J'_k \\ A-\leftrightarrow A+}} K(f_\ell \leftarrow f_k) \right). \qquad (9)$$

However, in the case of the ${}^{R}Q_0$ branch of CH_3Br, the rotational energies of A– and A+ levels of the upper state are very close, contrary to CH_3Cl, so that this refinement does not change the value of the right member of Eq. (8). Therefore, only A– ↔ A– collisional relaxations in the upper state have been considered to simplify the calculation. To ensure the convergence of the sums in Eq. (8), they were calculated with J_ℓ up to 80. For some levels with high rotational quantum number values, the level energies have been extrapolated using the spectroscopic constants given in [1,2].

The values obtained for a_1, a_2, a_3, and a_4 are given in Table 2, and the validity of the model is demonstrated on Fig. 2 showing the quality of the N_2- and self-broadening coefficients calculated in such a way.

The coefficients $A_{\ell,k}$ in Eq. (5) depend on the considered band and on the buffer gas, so that we have to determine the parameters A_{N_2} and A_{CH_3Br}, in addition to a_1, a_2, a_3 and a_4. Each parameter was determined from a single experimental spectrum, namely the spectrum at 849.8 hPa for N_2-perturbed CH_3Br, and the spectrum at 212.5 hPa for self-perturbed CH_3Br. This was done by successive estimations, and we found A_{N_2} = 0.70 and A_{CH_3Br} = 0.75. For all Q branches, the relaxation operators $\mathbf{W}_{CH_3Br/CH_3Br}$ and $\mathbf{W}_{CH_3Br/N_2}$ have then been calculated from the set of parameters of Table 2, using Eqs. (5-7) and the parameters A_{N_2} and A_{CH_3Br}. The broadening parameters calculated from the off-diagonal elements and the sum rule, are not perfect, especially for the Q branches with $K \neq 0$ (for which the broadening coefficients are different from those of the ${}^{R}Q_0$ branch (see Ref. [2])). The renormalization procedure [17,21] has been applied to the off-diagonal terms, in order to satisfy exactly the sum rule. Finally, note that two types of calculations of the absorption coefficient will be made: performing the direct calculation of Eq. (1) through the inversion of the relaxation operators $\mathbf{W}_{CH_3Br/CH_3Br}$ and $\mathbf{W}_{CH_3Br/N_2}$, and using the first order Rosenkranz profile [22].

FORTRAN codes have been written to generate the four relaxation operators $\mathbf{W}_{CH_3{}^{79}Br/CH_3Br}$, $\mathbf{W}_{CH_3{}^{81}Br/CH_3Br}$, $\mathbf{W}_{CH_3{}^{79}Br/N_2}$, and $\mathbf{W}_{CH_3{}^{81}Br/N_2}$, and to perform a direct calculation of the absorption coefficient. Considering one isotopologue of CH_3Br as the

absorbing gas, and the other isotopologue and N_2 as buffer gases, Eq. (1) becomes, for example in the case of a $CH_3{}^{79}Br$ transitions

$$\alpha\left(\sigma, P_{CH_3{}^{79}Br}, P_{N_2}, T\right) = \frac{8\pi^2\sigma}{3hc}\left[1-\exp\left(-hc\sigma/k_B T\right)\right] \times P_{CH_3{}^{79}Br} \times \sum_k \sum_\ell \rho_k(T) d_k d_\ell \, \mathrm{Im}\left\langle\left\langle \ell \left| \left[\boldsymbol{\Sigma} - \mathbf{L_0} - \mathrm{i}\left(P^{tot}_{CH_3Br} \times \mathbf{W}_{CH_3{}^{79}Br/CH_3Br}(T) + P_{N_2} \times \mathbf{W}_{CH_3{}^{79}Br/N_2}(T)\right)\right]^{-1} \right| k \right\rangle\right\rangle. \quad (10)$$

with $P^{tot}_{CH_3Br}$ the total pressure of CH_3Br, not to be confused with the partial pressures of the specific absorbing isotopologues. Results obtained by the direct calculation are presented in Section 4.

In order to simplify computations for possible atmospheric applications, the absorption coefficient was also calculated using the Rosenkranz profile [22]. Expanding Eq. (1) to first order, we obtain, e.g. in the case of $CH_3{}^{79}Br$ transitions

$$\alpha(\sigma, P_{CH_3{}^{79}Br}, P_{N_2}, T) = \frac{1}{\pi} P_{CH_3{}^{79}Br} \sum_k S_k(T) \frac{\sigma}{\sigma_k} \frac{\gamma_k + (\sigma-\sigma_k) Y_k}{(\sigma-\sigma_k)^2 + \gamma_k{}^2}, \quad (11)$$

where Y_k is a line-mixing parameter representing the coupling between line k of $CH_3{}^{79}Br$ and all other lines of the same branch. The Y_k's are given by

$$Y_k = 2\sum_{\ell \neq k} \frac{d_\ell}{d_k} \frac{\left\langle \langle \ell | P^{tot}_{CH_3Br} \times \mathbf{W}_{CH_3{}^{79}Br/CH_3Br}(T) + P_{N_2} \times \mathbf{W}_{CH_3{}^{79}Br/N_2}(T) | k \rangle \right\rangle}{\sigma_k - \sigma_\ell} = P^{tot}_{CH_3Br} \times Y_k^{CH_3{}^{79}Br/CH_3Br} + P_{N_2} \times Y_k^{CH_3{}^{79}Br/N_2} \quad (12)$$

As an example, Fig. 3 presents the values of $Y_k^{CH_3{}^{81}Br/N_2}$ for the ${}^RQ_0$ branch *vs* the J rotational quantum number, in unit of atm^{-1}. These values were found very close for the two isotopologues. At this stage of the work, it is interesting to discuss qualitatively these values and to compare them with those obtained by Chackerian et al [9] for another symmetric top molecule, CH_3Cl. Figure 3 shows that the values we obtained for CH_3Br have a very regular

rotational dependence, whereas the values obtained for CH_3Cl [9] exhibit strong irregularities. This is due to the fact that CH_3Cl, which is lighter than CH_3Br, has a more spaced and irregular pattern of rotational levels than CH_3Br. Furthermore, strong positive values have been found for low J lines of CH_3Cl, whereas we found them negative for CH_3Br. This is obviously because the studied Q branch of CH_3Cl extends towards high wavenumbers, whereas the Q branches of CH_3Br extend towards low wavenumbers. It is worth noticing that the Y_k values of low J lines, which strongly depend upon pressure-broadening coefficients difficult to measure for such lines, can have large uncertainties (estimated up to about 10%). We will show the efficiency of the Rosenkranz profile in the next section.

4. Spectra calculations and discussion

The calculated spectra were obtained as follows. First, due to the broad unresolved branches or observed features, it was not necessary to take into account the apparatus function. Absorption coefficients due to the two $CH_3{}^{79}Br$ and $CH_3{}^{81}Br$ isotopologues were added. Uncoupled lines present in the studied spectral domains were also taken into account in the calculation of the total absorption coefficient, their contribution being calculated using a Lorentz profile. Because of the large values of the self broadening compared with the N_2 broadening, the self broadening has been taken into account, although the partial pressures of CH_3Br that we used were quite small as compared to the N_2 ones. The total broadening coefficient of a CH_3Br transition is then given by the usual linear mixing rule

$$\gamma(k) = P_{N_2} \times \gamma_{N_2}(k) + P^{tot}_{CH_3Br} \times \gamma_{self}(k) . \qquad (13)$$

In Eq. (13), $\gamma_{N_2}(k)$ and $\gamma_{self}(k)$ are respectively the N_2- and self-broadening coefficients from Ref. [2]. Because of the high pressures, it was not necessary to take into account the Doppler broadening for CH_3Br in this spectral region.

4.1. Line-mixing effects on self-broadened CH_3Br spectra

The a_1, a_2, a_3, and a_4 parameters reported in Table 2 for self-perturbed CH_3Br were used, as also the value found for A_{CH_3Br}, so that no parameters were adjusted at this stage of the calculations. Because of the strong electric dipole moment of the CH_3Br molecule, the CH_3Br / CH_3Br collisions are more efficient than the CH_3Br / N_2 ones, leading to self-broadening coefficients very much larger than N_2-broadening ones [2], and consequently to a stronger line mixing (even at low pressure), more difficult to model. As example, Fig. 4 presents results obtained for the ${}^RQ_0$ branch at three pressures. The absorption spectra have been plotted with transmission as ordinate, and the continuous background was considered a constant adjusted along each plotted spectral domain.

The effects of the line mixing on pure CH_3Br spectra are well observed in the residuals of the fit. Where line mixing occurs, the characteristic signature obtained using a sum of Lorentz or Voigt profiles is considerably reduced when performing the direct calculation of Eq. (9). Note that the weak oscillation in the residuals of the lowest pressure spectrum at 67 hPa (Fig. 4a), observable in the tail of the *Q* branch towards low wavenumbers, should not be attributed to line-mixing effects, but merely to slight discrepancies between the experimental line positions and intensities, and those computed in [2] and used in our calculations. At higher pressure, the involved features are no longer resolved (Figs. 4b,c), and the oscillating signature disappears.

4.2. Line-mixing effects on the ${}^RQ_0$ branch of N_2-broadened CH_3Br spectra

Figure 5 presents results obtained in the ${}^RQ_0$ branch region, for three different pressures of nitrogen. As for self-perturbed spectra, these results confirm that neglecting line mixing leads to large errors, whereas our model gives satisfactory predictions. Comparisons between the experimental spectra and the ones calculated using a sum of Lorentz profiles show the absorption transfer from the regions of weak absorption to those of strong absorption. Outside the *Q* branch, where there is no noticeable line mixing, the experimental spectra and those calculated using a sum of Lorentz profiles are superimposed. Examining more accurately Fig. 5, one observes a very weak channeled spectrum in the residuals (period

around 4 cm^{-1}), having an experimental origin (see Section 1). Because of its weakness, we did not try to model and remove such an irregular and faint effect, which should be distinguished from line-mixing effects that would have not been taken into account.

Note that the residuals obtained with spectra calculated with the Rosenkranz profile are quasi-superimposed to those obtained by the full calculation performed directly from Eq. (10). Only a slight discrepancy appears just at the branch head inside a very narrow spectral domain, where the Rosenkranz profile underestimates the line mixing, whereas the full calculation overestimates them. This first order line-mixing profile, easy and quick to compute from Eqs. (11, 12), could therefore be used in this range of pressures, instead of the full calculation (Eq. (10)).

4.3. Line-mixing effects on other $^{R}Q_{K}$ and $^{P}Q_{K}$ branches of N_2-broadened CH_3Br spectra

The model was applied to all branches of the ν_6 band and gave a good agreement with experimental spectra at different pressures. We present here representative examples of $^{R}Q_{K}$ and $^{P}Q_{K}$ branches. Their spectral structures are significantly different from that of $^{R}Q_{0}$, so that they enable a meaningful test of our approach. Let us recall that the parameters a_1, a_2, a_3, and a_4 were determined from the pressure-broadening coefficients of $^{R}Q_{0}$ lines, and are now fixed to the same values for the other branches. Note that the renormalization procedure was necessary for these branches, since the diagonal elements of **W** have now to be identified with the N_2-broadening coefficients specific to each branch, which can differ from those of $^{R}Q_{0}$ lines [2].

Comparisons between experimental and calculated spectra are shown on Figs. 1, 6, and 7. As expected, although line-mixing effects in these branches are smaller than in the $^{R}Q_{0}$ branch, the disagreements between the experimental data and the spectra calculated using the sum of Lorentz profiles remain important and qualitatively similar to that of $^{R}Q_{0}$. As shown on these figures, spectra calculated with our model are in good agreement with experiment.

The slight difference appearing between measured and calculated spectra in the branch heads at high N_2 pressure is probably due to inter-branch line-mixing effects that could be determined by a direct adjustment of a calculated spectrum to the experimental one,

as done for CH_4 in Ref. [14]. However, the CH_3Br spectrum is very crowded and contains numerous weak high *J* lines and some *Q* branches of the $2\nu_6$ - ν_6 hot band not calculated in Ref. [2], but observable in the residuals of Fig. 1b. Therefore, such a direct adjustment of line-mixing parameters from an experimental spectrum could not be accurately performed at the present time. Though these hot bands can not receive an accurate spectroscopic treatment, it is however possible to roughly model them for possible applications, and therefore to decrease slightly the residuals, as has been done on Fig. 1. For that, the *Q* branches of the ν_6 band have shifted and rescaled to simulate those of the $2\nu_6$ ν_6 hot band.

6. Conclusion

Line-mixing effects have been calculated in the ν_6 band of the main isotopologues of methyl bromide, N_2-perturbed and self-perturbed at room temperature. The model used is based on the use of the state-to-state rotational cross-sections calculated by a statistical modified exponential-gap fitting law, that depends on a few adjusted empirical parameters. Comparisons performed between experimental and calculated spectra, under atmospheric pressure conditions (0.2 - 1 atm), demonstrate the efficiency/effectiveness of the model to noticeably decrease the large systematic errors that would affect the treatment of experimental spectra if line mixing was disregarded. Furthermore, the simple first order Rosenkranz profile appeared precise enough for quick calculations.

There exists a strong demand to include accurate spectroscopic data on the methyl bromide molecule in atmospheric databases as HITRAN [23] and GEISA [24], especially for the ν_6 band, which is located in an atmospheric window, and could be observed in long path solar occultation spectra at sunset or sunrise. The ${}^{R}Q_0$ branch particularly, seems well suited for such studies, being located in a micro window, between two carbon dioxide lines and two water vapor lines. That is why we plan to record new spectra at temperatures of atmospheric interest, in order to get a better knowledge of the N_2-broadening and line-mixing coefficients of CH_3Br.

Acknowledgments

Dr. J.-M. Hartmann and Pr. V. Dana are gratefully acknowledged for very helpful suggestions and discussions throughout this work. All the experimental spectra have been recorded by Emilie Brunetaud.

References

[1] Brunetaud É, Kleiner I, Lacome N. Line intensities in the ν_6 fundamental band of CH_3Br at 10 µm. J Mol Spectrosc 2002;216:30-47.

[2] Jacquemart D, Kwabia Tchana F, Lacome N, Kleiner I. A complete set of line parameters for CH_3Br in the 10-µm spectral region. JQSRT, in press.

[3] Ben-Reuven A. Impact broadening of microwave spectra. Phys Rev 1966;145:7-22.

[4] Lévy A, Lacome N, Chackerian C, Jr. Collisional line-mixing. In: Spectroscopy of the Earth's atmosphere and interstellar medium. Rao KN, Weber A, Eds. Academic Press, Inc. 1992; pages 261-337.

[5] Grigoriev IM, Le Doucen R, Benidar A, Filippov NN, Tonkov MV. Line-mixing effects in the ν_3 parallel absorption band of CH_3F perturbed by rares gases. JQSRT 1997;58:287-99.

[6] Thibault F, Boissoles J, Grigoriev IM, Filippov NN, Tonkov MV. Line-mixing effects in the ν_3 band of CH_3F in helium: Experimental band shapes and ECS analysis. Eur Phys J D 1999 ;6 :343-53.

[7] Hartmann JM, Bouanich JP, Boulet C, Blanquet G, Walrand J, Lacome N. Simple modelling of Q branch absorption - II: Application to molecules of atmospheric interest (CFC-22 and CH_3Cl). JQSRT 1995;54:723-35.

[8] Frichot F, Lacome N, Harmann JM. Pressure and temperature dependences of absorption in the ν_5 $^RQ_0$ branch of CH_3Cl in N_2: Measurements and modelling. J Mol Sectrosc 1996;178:52-8.

[9] Chackerian C, Jr., Brown LR, Lacome N, Tarrago G. Methyl chloride ν_5 region lineshape parameters and rotational constants for the ν_2, ν_5, and $2\nu_3$ vibrational bands. J Mol Spectrosc 1998;191:148-57.

[10] Wartewig S. IR and Raman Spectroscopy: Fundamental Processing. Wiley-VCH, Weinheim, 2003.

[11] Mertz L. Transformations in Optics. Wiley, New York, 1965.

[12] Griffiths PR, deHaseth JA. Fourier Transform Infrared Spectrometry. Wiley, New York, 1986.

[13] Pieroni D, Nguyen Van Thanh, Brodbeck C, Claveau C, Valentin A, Hartmann JM, Gabard T, Champion JP, Bermejo D, Domenech JL. Experimental and theoretical study of line-mixing in methane spectra. I. The N_2-broadened ν_3 band at room temperature. JQSRT 1999; 110:7717-7732.

[14] Tran H, Flaud PM, Gabard T, Hase F, von Clarmann T, Camy-Peyret C, Payan S, Hartmann JM. Model, software and database for line-mixing effects in the ν_3 and ν_4 bands of CH_4 and tests using laboratory and planetary measurements - I: N_2 (and air) broadening and the Earth atmosphere. JQSRT 2006;101:284-305.

[15] Rahn LA, Palmer RE. Studies of nitrogen self-broadening at high temperature with inverse Raman spectroscopy. J Opt Soc Am B 1986;3:1164-9.

[16] Herlemont F, Thibault J, Lemaire J. Study of rotational relaxation in CH_3Br by infrared-microwave double resonance. Chem Phys Let 1976;41:466-9.

[17] Niro F, Boulet C, Hartmann JM. Spectra calculations in central and wing region of CO_2 IR bands between 10 and 20 μm - I: Model and laboratory measurements. JQSRT 2004;88:483-98.

[18] Everitt HO, de Lucia F. Rotational energy transfer in CH_3F: The $\Delta J=n$, $\Delta K=0$ processes. J Chem Phys 1990;92:6480-91.

[19] Frenkel L, Marantz H, Sullivan T. Spectroscopy and collisional transfer in CH_3Cl by microwave-laser double resonance. Phys Rev A 1971;3:1640-51.

[20] Pape TW, De Lucia FC, Skatrud DD. Time resolved double resonance study of J and K changing rotational collision processes in CH_3Cl. J Chem Phys 1994;100:5666-83.

[21] Tran H, Boulet C, Hartmann JM. Line-mixing and collision-induced absorption by oxygen in the A band: Laboratory measurements, model, and tools for atmospheric spectra computations. J Geophys Res 2006;111,D15210:1-14.

[22] Rosenkranz PW. Shape of the 5 mm oxygen band in the atmosphere. IEEE Trans Antennas Propag 1975;AP-23:498-506.

[23] Rothman LS, Jacquemart D, Barbe A, Benner DC, Birk M, Brown LR, Carleer MR, Chackerian Jr C, Chance K, Coudert LH, Dana V, Devi VM, Flaud JM, Gamache RR, Goldman A, Hartmann JM, Jucks KW, Maki AG, Mandin JY, Massie ST, Orphal J, Perrin A, Rinsland CP, Smith MAH, Tennyson J, Tolchenov RN, Toth RA, Vander Auwera J, Varanasi P, Wagner G. The HITRAN 2004 molecular spectroscopic database. JQSRT 2005;96:139-204.

[24] Jacquinet-Husson N, Scott NA, Chedin A, Garceran K, Armante R, Chursin AA, Barbe A, Birk M, Brown LR, Camy-Peyret C, Claveau C, Clerbaux C, Coheur PF, Dana V, Daumont L, Debacker-Barilly MR, Flaud JM, Goldman A, Hamdouni A, Hess M, Jacquemart D, Köpke P, Mandin JY, Massie S, Mikhailenko S, Nemtchinov V, Nikitin A, Newnham D, Perrin A, Perevalov VI, Régalia-Jarlot L, Rublev A, Schreier F, Schult I, Smith KM, Tashkun SA, Teffo JL, Toth RA, Tyuterev VIG, Vander Auwera J, Varanasi P, Wagner G. The 2003 Edition Of The GEISA/IASI spectroscopic database. JQSRT 2005;95:429-67.

Table 1. Experimental conditions and characteristics of the recorded spectra

Unapodized apparatus function

Spectra 1-4	Maximum optical path difference	450 cm
	FWHM	$\approx 1 \times 10^{-3}$ cm^{-1}
Spectra 5-6	Maximum optical path difference	125 cm
	FWHM	$\approx 4 \times 10^{-3}$ cm^{-1}

Absorbing sample

Natural CH_3Br	50.54 % of $CH_3{}^{79}Br$
	49.46 % of $CH_3{}^{81}Br$
	(about 1 % of ^{13}C isotopologues neglected)
Stated purity	99.50 %

Experimental conditions

S/N ratio	≈ 100

#	CH_3Br pressure (hPa)	N_2 pressure (hPa)	Absorption path (cm)
1	66.5	0	30
2	109.4	0	30
3	212.5	0	30
4	2.01	287.1	415
5	53.1	550.9	30
6	49.3	849.8	30

Table 2: Parameters of the MEG model obtained for CH_3Br/N_2 and CH_3Br/CH_3Br

MEG law parameter	CH_3Br/N_2	CH_3Br/CH_3Br
a_1	0.00708	0.1006
a_2	2.589	0.1883
a_3	1.067	20.81
a_4	0.571	0.891

Fig. 1. $P(CH_3Br)$ = 49.3 hPa, $P(N_2)$ = 849.8 hPa, L = 30 cm. In the upper panel, the experimental spectrum is plotted. The panels of residuals show the differences between the experimental spectrum and a spectrum calculated without taking into account line-mixing (a), with line-mixing taken into account, remaining features in the residuals being due to hot bands and high *J* lines of ν_6 (b), and same as (b) but with hot bands roughly taken into account (c).

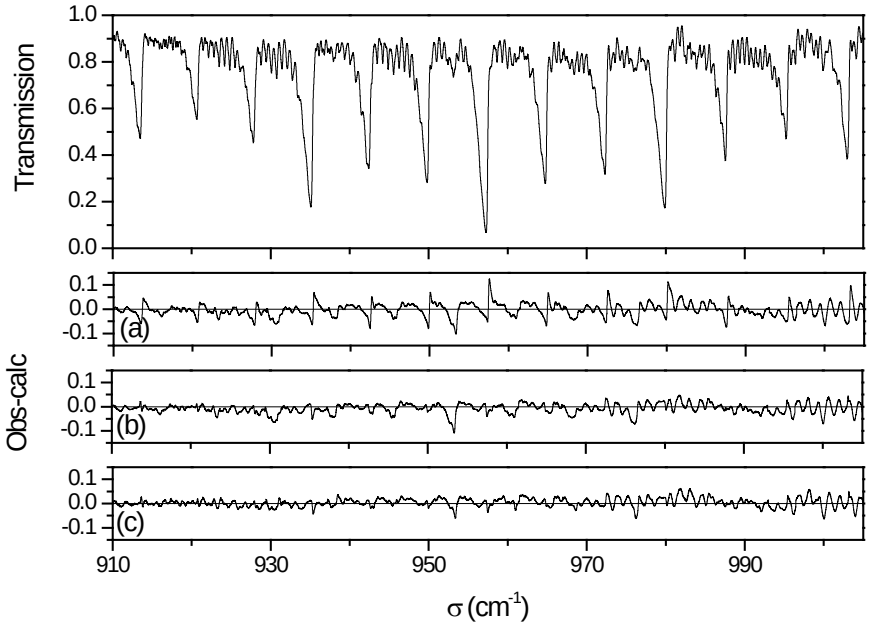

Fig. 2. Comparison between broadening coefficients of CH_3Br in the ${}^{R}Q_0$ branch given by [2] (solid square) and those calculated by the MEG model (solid curve). Note that the broadening coefficients calculated for $CH_3{}^{79}Br$ and $CH_3{}^{81}Br$ are not distinguishable from the solid curve shown. *J* is the rotational quantum number of the lower level of the radiative transition.

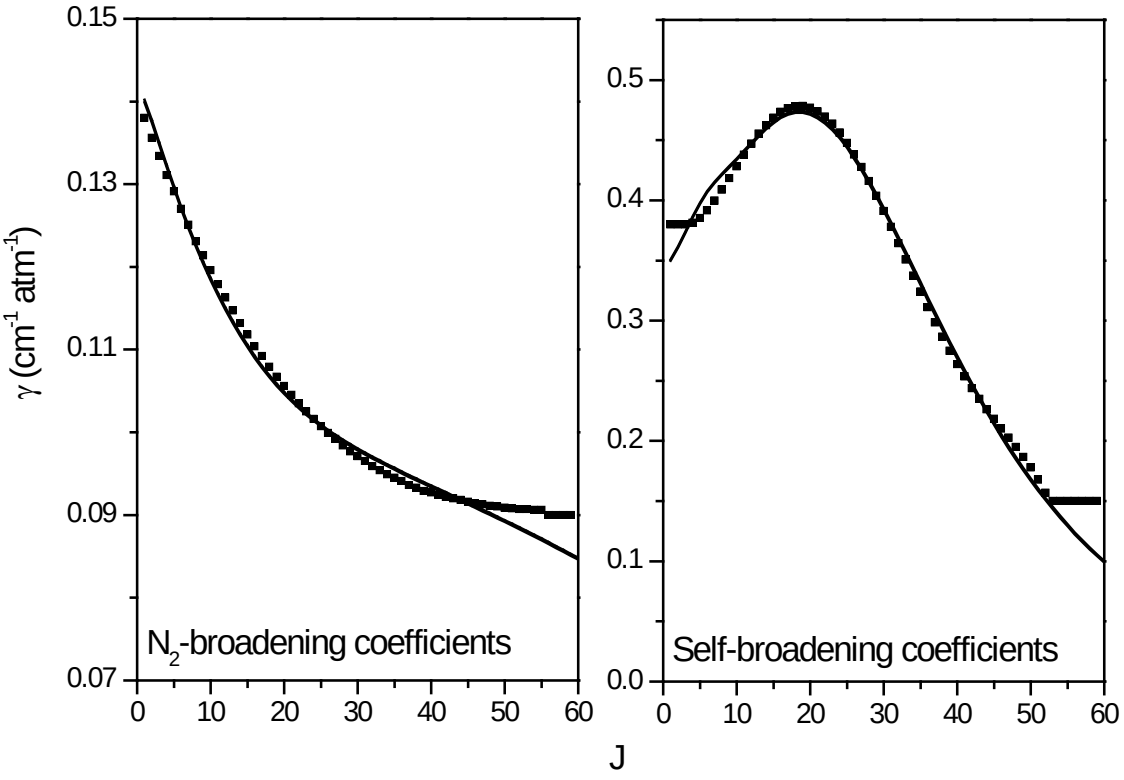

Fig. 3. First order line-mixing parameters $Y_k^{CH_3{}^{81}Br/N_2}$ of the Rosenkranz profile *vs* the rotational quantum number *J* of the lower state, for the ν_6 $^RQ_0$ branch of $CH_3{}^{81}Br$.

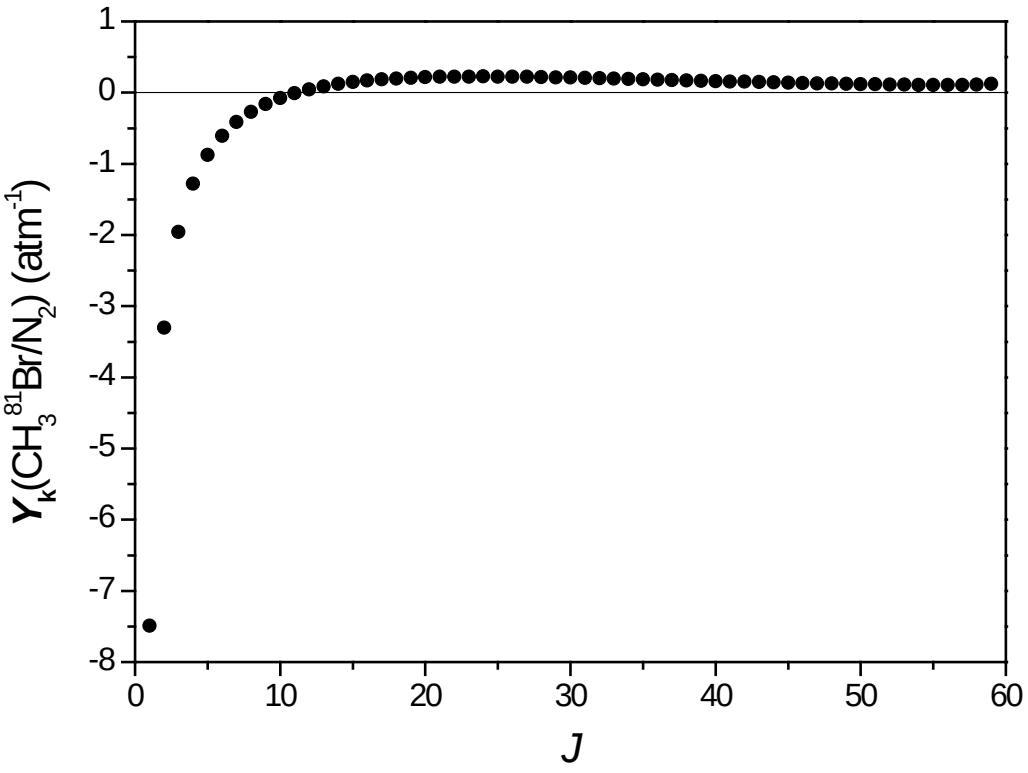

Fig. 4. Comparison between the CH_3Br/CH_3Br transmission spectra in the ${}^{R}Q_0$ branch region calculated without line-mixing (—) and experimental values (•). For the sake of clarity, all experimental values have not been plotted. These results have been obtained at room temperature with an absorbing path length of 30 cm and for 66.5 hPa (a), 109.4 hPa (b), and 212.5 hPa (c) of CH_3Br in natural abundances. The upper panels of residuals show the differences between the experimental spectra and spectra calculated without line-mixing, and the lower panels the differences between the experimental spectra and line-mixing full calculation spectra.

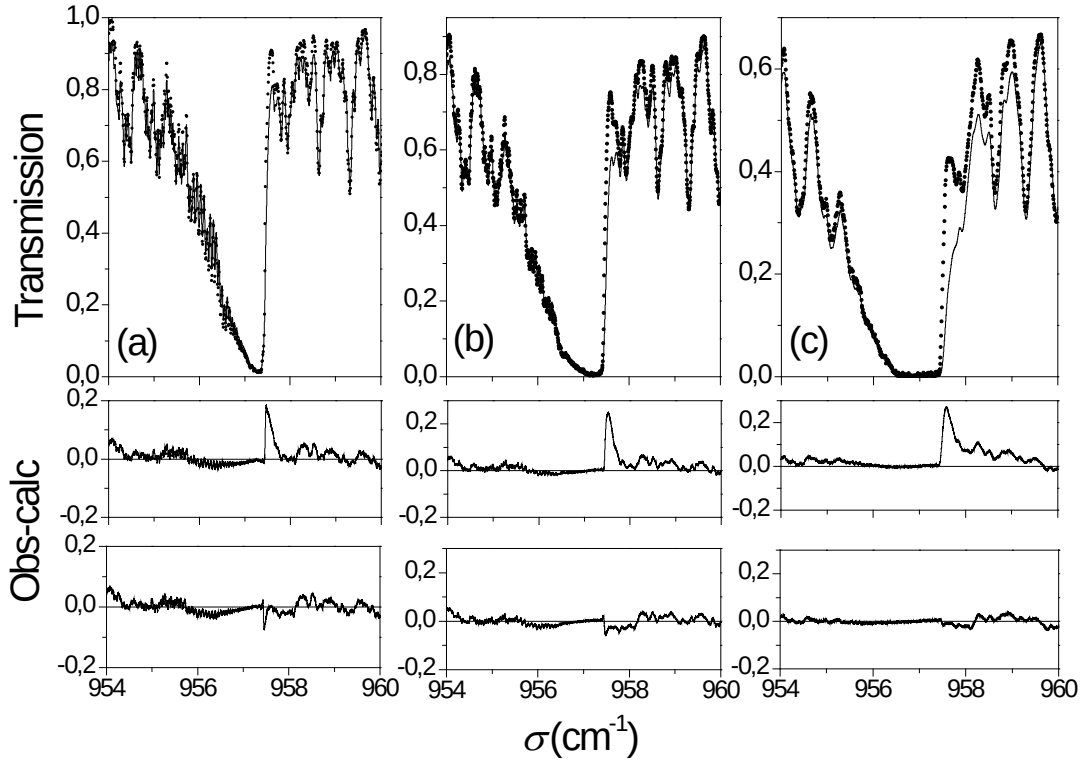

Fig. 5. Comparison between the CH_3Br/N_2 transmission spectra in the ${}^{R}Q_0$ branch region calculated without line-mixing (—) and the experimental values (•). These results have been obtained at room temperature, for: 2 hPa of CH_3Br diluted in 287.1 hPa of N_2 with an absorbing path length of 415 cm (a), 53.1 hPa of CH_3Br diluted in 550.9 hPa of N_2 with an absorbing path length of 30 cm (b), 49.3 hPa of CH_3Br diluted in 849.8 hPa of N_2 with an absorbing path length of 30 cm (c). The upper panels of residuals show the differences between the experimental spectra and spectra calculated with a sum of Lorentz profiles, the middle panels the differences between the experimental spectra and spectra calculated with a Rosenkranz profile, and the lower panels the differences between the experimental spectra and line-mixing full calculation spectra.

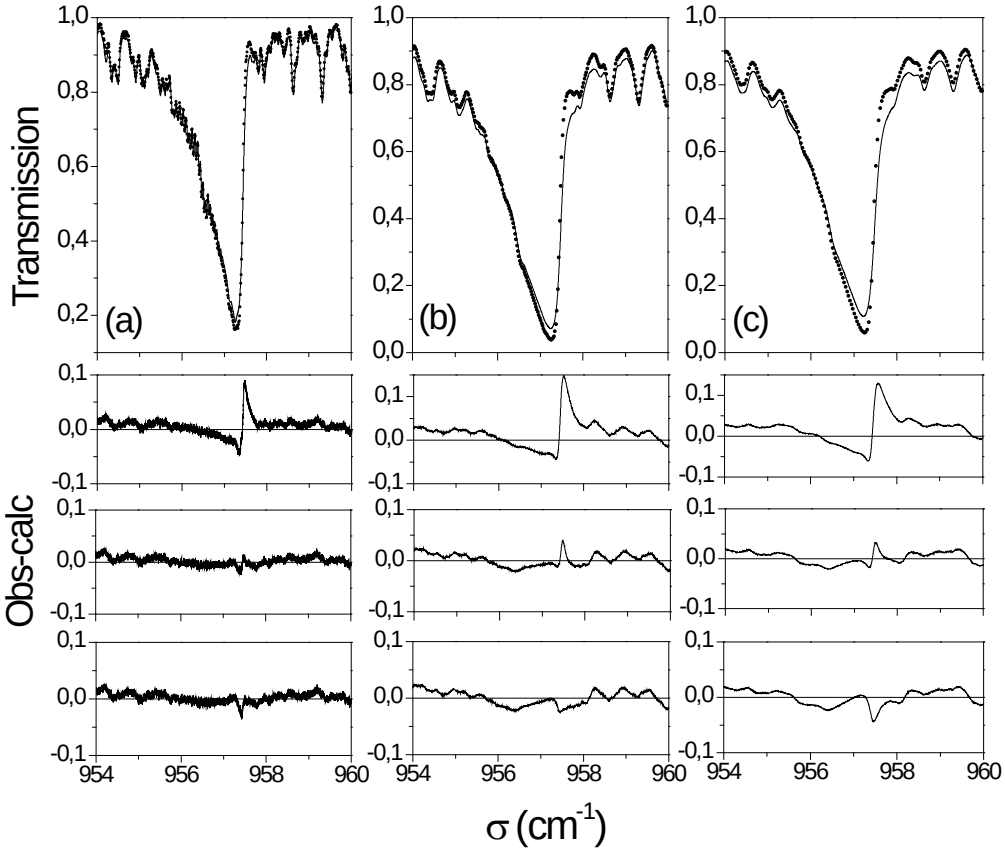

Fig. 6 : Comparison between the transmissions of CH_3Br/N_2 in the ${}^{P}Q_6$ (a) and ${}^{P}Q_3$ (b) branches regions calculated with (—) and without (---) line-mixing, and the measured values (•). These results have been obtained at room temperature, for 53.1 hPa of CH_3Br diluted in 550.9 hPa of N_2, and for an absorbing path length of 30 cm.

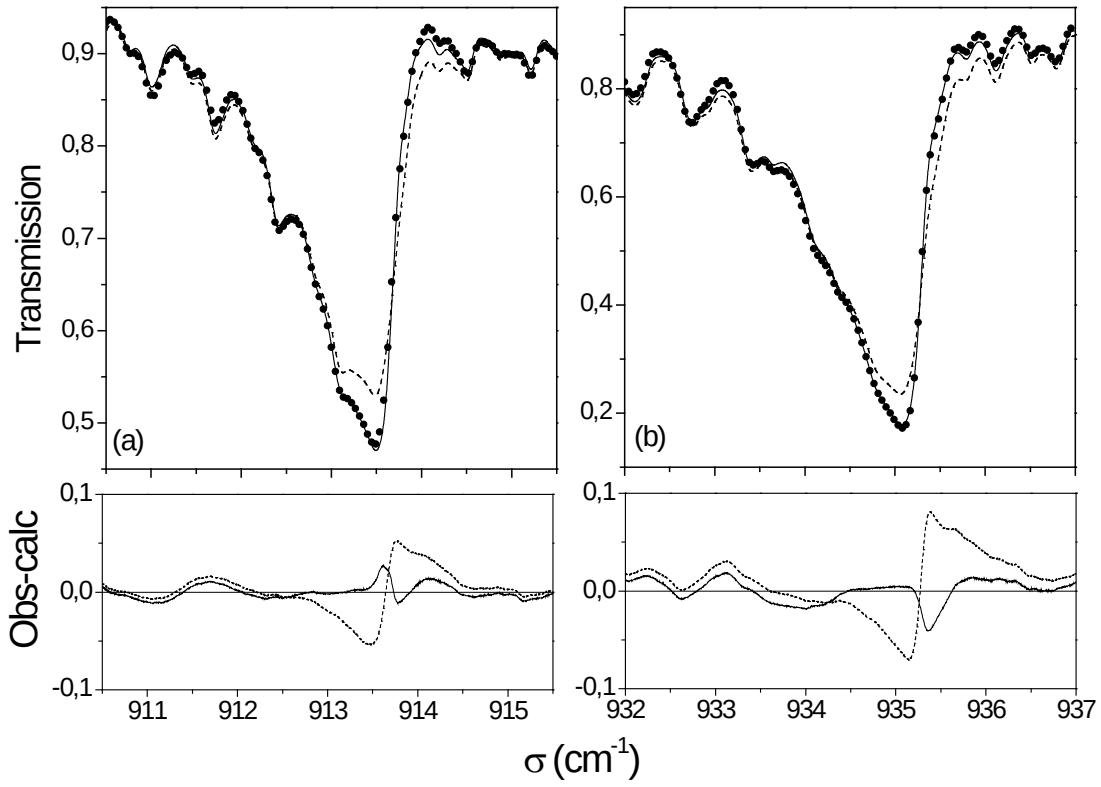

Fig. 7. Comparison between the transmissions of CH_3Br/N_2 in the ${}^{R}Q_1$ (a) and ${}^{R}Q_3$ (b) branches regions calculated with (—) and without (---) line-mixing, and the measured values (•). These results have been obtained at room temperature, for 49.3 hPa of CH_3Br diluted in 849.8 hPa of N_2, and for an absorbing path length of 30 cm.